JOMH
Journal of Men's Health

J. Mens. Health **2022**; 18(1): 025
http://doi.org/10.31083/j.jomh1801025

Original Research

A prognostic index model for assessing the prognosis of ccRCC patients by using the mRNA expression profiles of *AIF1L*, *SERPINC1* and *CES1*

Song Zheng[1], Zihao Chen[2], Jianhui Chen[1], Rong Liu[1], Mei Song[3], Angchao Ye[4], Shaoxing Zhu[5,6,7], Hua Wang[5], Zongping Wang[5], Fangyin Li[5], Jinhan Lou[5], Yaping Chen[5], Fang Fang[5], Chunmei Wen[5], Jing Zhang[5], Bilan Xue[5], He Wang[8], Jianmin Lou[8], Weizhong Cai[1,*], Yaoyao Wu[8,*], Yipeng Xu[5,6,7,*]

[1]Department of Urology, Fujian Medical University Union Hospital, 350001 Fuzhou, Fujian, China
[2]Department of Urology, Southern Medical University, 510515 Guangzhou, Guangdong, China
[3]Department of Ultrasound, The Cancer Hospital of the University of Chinese Academy of Sciences, Zhejiang Cancer Hospital, 310022 Hangzhou, Zhejiang, China
[4]Department of Neurology, Integrated Traditional Chinese and Western Medicine Hospital of Linping District, 310005 Hangzhou, Zhejiang, China
[5]Department of Urology, The Cancer Hospital of the University of Chinese Academy of Sciences, Zhejiang Cancer Hospital, 310022 Hangzhou, Zhejiang, China
[6]The Key Laboratory of Zhejiang Province for Aptamers and Theranostics, Chinese Academy of Sciences, 310063 Hangzhou, Zhejiang, China
[7]Institute of Basic Medicine and Cancer (IBMC), Chinese Academy of Sciences, 310063 Hangzhou, Zhejiang, China
[8]The Second Clinical Medical College, Zhejiang Chinese Medical University, 310059 Hangzhou, Zhejiang, China
*Correspondence: xuyp1631@zjcc.org.cn (Yipeng Xu); yaoyaowu511@126.com (Yaoyao Wu); xiaoyaoyou1983@126.com (Weizhong Cai)
Submitted: 13 October 2021 Accepted: 29 November 2021 Published: 19 January 2022

Abstract

Background: Kidney carcinoma is a major cause of carcinoma-related death, with the prognosis for advanced or metastatic renal cell carcinoma still very poor. The aim of this study was to investigate feasible prognostic biomarkers that can be used to construct a prognostic index model for clear cell renal cell carcinoma (ccRCC) patients. **Methods**: The mRNA expression profiles of ccRCC samples were downloaded from the The Cancer Genome Atlas (TCGA) dataset and the correlation of *AIF1L* with malignancy, tumor stage and prognosis were evaluated. Differentially expressed genes (DEGs) between *AIF1L*-low and *AIF1L*-high expression groups were selected. Those with prognostic value as determined by univariate and multivariate Cox regression analysis were then used to construct a prognostic index model capable of predicting the outcome of ccRCC patients. **Results**: The expression level of *AIF1L* was lower in ccRCC samples than in normal kidney samples. *AIF1L* expression showed an inverse correlation with tumor stage and a positive association with better prognosis. ccRCC samples were divided into high- and low-expression groups according to the median value of *AIF1L* expression. In the *AIF1L*-high expression group, 165 up-regulated DEGs and 601 down-regulated DEGs were identified. Three genes (*AIF1L*, *SERPINC1* and *CES1*) were selected following univariate and multivariate Cox regression analysis. The hazard ratio (HR) and 95% confidence intervals (CI) for these genes were: *AIF1L* (HR = 0.83, 95% CI: 0.76–0.91), *SERPINC1* (HR = 1.33, 95% CI: 1.12–1.58), and *CES1* (HR = 0.87, 95% CI: 0.78–0.97). A prognostic index model based on the expression level of the three genes showed good performance in predicting ccRCC patient outcome, with an area under the ROC curve (AUC) of 0.671. **Conclusion**: This research provides a better understanding of the correlation between *AIF1L* expression and ccRCC. We propose a novel prognostic index model comprising *AIF1L*, *SERPINC1* and *CES1* expression that may assist physicians in determining the prognosis of ccRCC patients.

Keywords: ccRCC; Prognostic index model; *AIF1L*; *SERPINC1*; *CES1*

1. Introduction

Kidney carcinoma is one of the three malignant tumors of the urinary system. It had a global incidence of approximately 431,000 new cases and was responsible for 179,000 related deaths in 2020 [1]. The incidence of kidney carcinoma is much higher in developed regions such as North America and Europe than in Asia and Africa [1,2]. Renal cell carcinoma (RCC) is the most normal histological subtype of kidney carcinoma and represents approximately 90% of all cases. ccRCC is the most common RCC subtype and accounts for 75% of cases [3]. Although the large majority of early, localized RCC can be cured by surgical treatment, the 5-year overall survival rate for advanced and metastatic RCC (mRCC) is only 5–10% [4]. Molecular-targeted therapeutic drugs such as Vascular endothelial growth factor (VEGF)/Vascular Endothelial Growth Factor Receptor (VEGFR) inhibitors and immunotherapy agents such as PD-1 antibodies have markedly improved the clinical prognosis of mRCC patients [5–8]. However, their long-term benefit for patient survival remains unsatisfactory [9,10]. The complexity of tumor heterogeneity and the clonal evolution of tumors ultimately leads to clinical drug resistance [11]. Advanced or metastatic RCC therefore remains as one of the most treatment-resistant cancer

types. In order to improve patient outcomes, there is an urgent need for well-defined diagnostic biomarkers that can be used for early detection, risk stratification, and to overcome drug resistance.

EF-hand (EFh) domain-containing proteins have been implicated in malignant progression [12]. Allograft inflammatory factor 1 (*AIF1*, also referred to as *IBA1*) contains Efh and plays a critical role in the initiation and progression of cancers [13–18]. *AIF1L* (allograft inflammatory factor 1-like, also referred to as *IBA2*) is a homolog of *AIF1* [19,20] and has a similar overall structure and molecular function [20]. Nevertheless, the two proteins may have diverse functions, as suggested by the different expression patterns seen in different tissues [21]. AIF1 is preferentially expressed in the spleen, tonsil, lymph node, thymus, and lung [22,23], whereas *AIF1L* is notably expressed in the kidney. A potential role for *AIF1L* in tumorigenesis of the kidney and the associated molecular mechanisms have yet to be described.

In the present study, *AIF1L* was found to be significantly downregulated in ccRCC. A total of 539 ccRCC tumors were clustered according to the median value of *AIF1L* expression value and separated into *AIF1L*-high and *AIF1L*-low expression group. Univariate and multivariate Cox regression analysis were then used to identify differentially expressed genes (DEGs) with prognostic value. A prognostic index model based on the expression levels of *AIF1L*, *SERPINC1*, and *CES1* was then constructed to predict clinical outcome and to guide treatment.

2. Methods

2.1 Data acquisition and pre-processing

Level three sequencing data and clinical follow-up data for 539 clear cell renal cell carcinoma (ccRCC) samples and 72 corresponding healthy kidney samples was extracted from the TCGA dataset. The Fragments Per Kilobase of exon model per Million mapped fragments (FPKM) expression profile was then converted to Transcripts Per Kilobase Million (TPM) based on the sum of expression of all genes in a sample being 100,000. The microarray gene expression profile and related clinical data for GSE40435 [24], containing 101 pairs of ccRCC and adjacent non-tumor renal tissue, was downloaded and used to validate the results of this study.

2.2 Correlation of AIF1L expression with malignancy, pathological stage, and prognosis

The students *t*-test was used to evaluate statistical differences in mRNA expression between ccRCC and normal tissues. Similarly, paired *t*-tests were applied between paired ccRCC and adjacent normal tissues. Differences in *AIF1L* expression between subgroups of various clinicopathological parameters were analyzed by the Kruskal-Wallis test. Survival curves for *AIF1L*-low and -high expression groups were plotted by Kaplan-Meier analysis and compared using log-rank tests.

2.3 Functional enrichment analysis based on differentially expressed genes (DEGs)

To identify genes associated with *AIF1L* expression, DEGs between the *AIF1L*-high and *AIF1L*-low groups were selected by the "edgeR" package in R language [25]. The median value for *AIF1L* expression was used to generate the *AIF1L*-high and *AIF1L*-low groups. The fold-change and *p* values were calculated for each gene. Genes with a log2 fold-change >1 and a p-value < 0.05 were selected as DEGs [26,27]. Functional enrichment analysis including Gene Ontology (GO) and the Kyoto Encyclopedia of Genes and Genomes (KEGG) 29 was conducted for these DEGs. Pathways with a p-value < 0.05 were regarded as statistically significant.

2.4 Construction of a prognostic index model

DEGs were further selected according to their prognostic value as determined by univariate and multivariate prognostic index Cox proportional hazard regression models [28]. The expression profiles of selected DEGs were then used to construct a prognostic index model. ccRCC patient samples were classified into high and low groups according to the prognostic index's median cut-off. Overall survival was studied using Kaplan-Meir analysis. The AUC was calculated to assess discrimination of the prognostic index model in the TCGA samples.

2.5 Statistical analysis

All statistical analyses were conducted using R language. Kaplan-Meier survival and univariate and multivariate analyses were performed using the R package "survival". ROC curves were plotted using the R package "survival ROC". In all statistical analyses, significance was accepted at a p-value < 0.05.

3. Results

3.1 AIF1L downregulation in ccRCC correlated with malignancy, advanced tumor stage and poor survival

To investigate the relationship between *AIF1L* and the malignant phenotype in ccRCC, transcriptome data for *AIF1L* in the TCGA dataset was analyzed for 539 ccRCC tumors and 72 normal kidney samples. *AIF1L* mRNA expression was markedly lower in ccRCC tissues compared to normal kidney samples (p-value < 0.001, Fig. 1A). The paired students *t*-test also showed that *AIF1L* expression was lower in ccRCC samples compared to matched normal samples (p-value < 0.001, Fig. 1B). Patients with advanced stages of ccRCC had significantly lower levels of *AIF1L* expression than patients with earlier stages (p-value < 0.001, Fig. 1C). Kaplan-Meier survival curves showed that patients with low *AIF1L* expression had significantly worse overall survival compared to those with high expression (p-value = 0.042, Fig. 1D). A significant difference was also observed for recurrence-free survival (p-value = 0.0017, Fig. 1E). An independent dataset (GSE40435) was

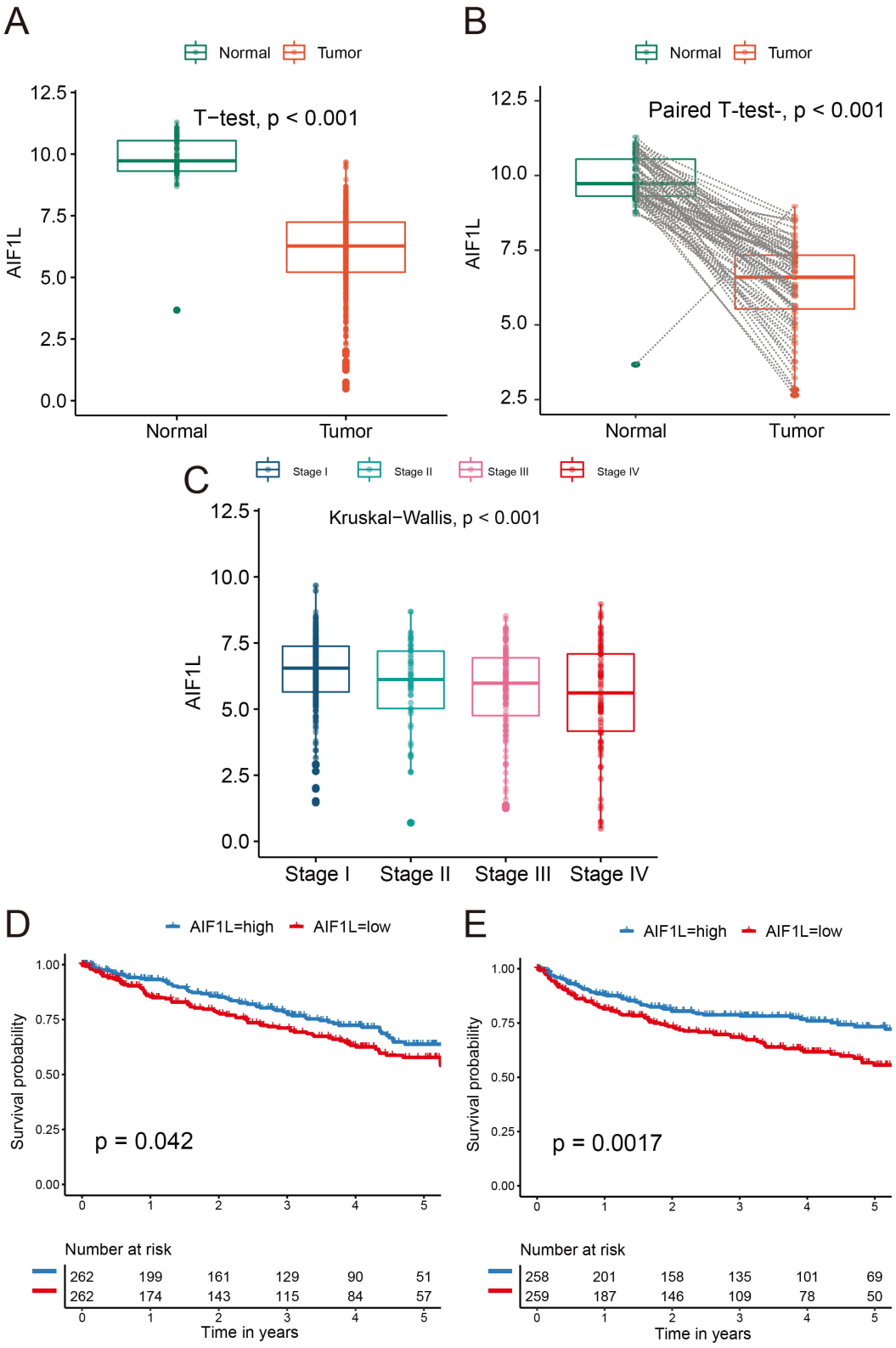

Fig. 1. Correlation of *AIF1L* expression with malignancy, tumor stage, and prognosis in ccRCC. (A) Student *t*-test result for the comparison of *AIF1L* expression between ccRCC and normal kidney samples from the TCGA dataset. (B) Paired *t*-test result for *AIF1L* expression between paired ccRCC and normal kidney samples from the TCGA dataset. (C) Kruskal-Wallis test result for *AIF1L* expression between Stage I, Stage II, Stage III and StageIV tumor samples. (D) Overall survival analysis for ccRCC samples from the TCGA dataset with high or low *AIF1L* expression. (E) Recurrence-free survival analysis for ccRCC samples from the TCGA dataset with high or low *AIF1L* expression.

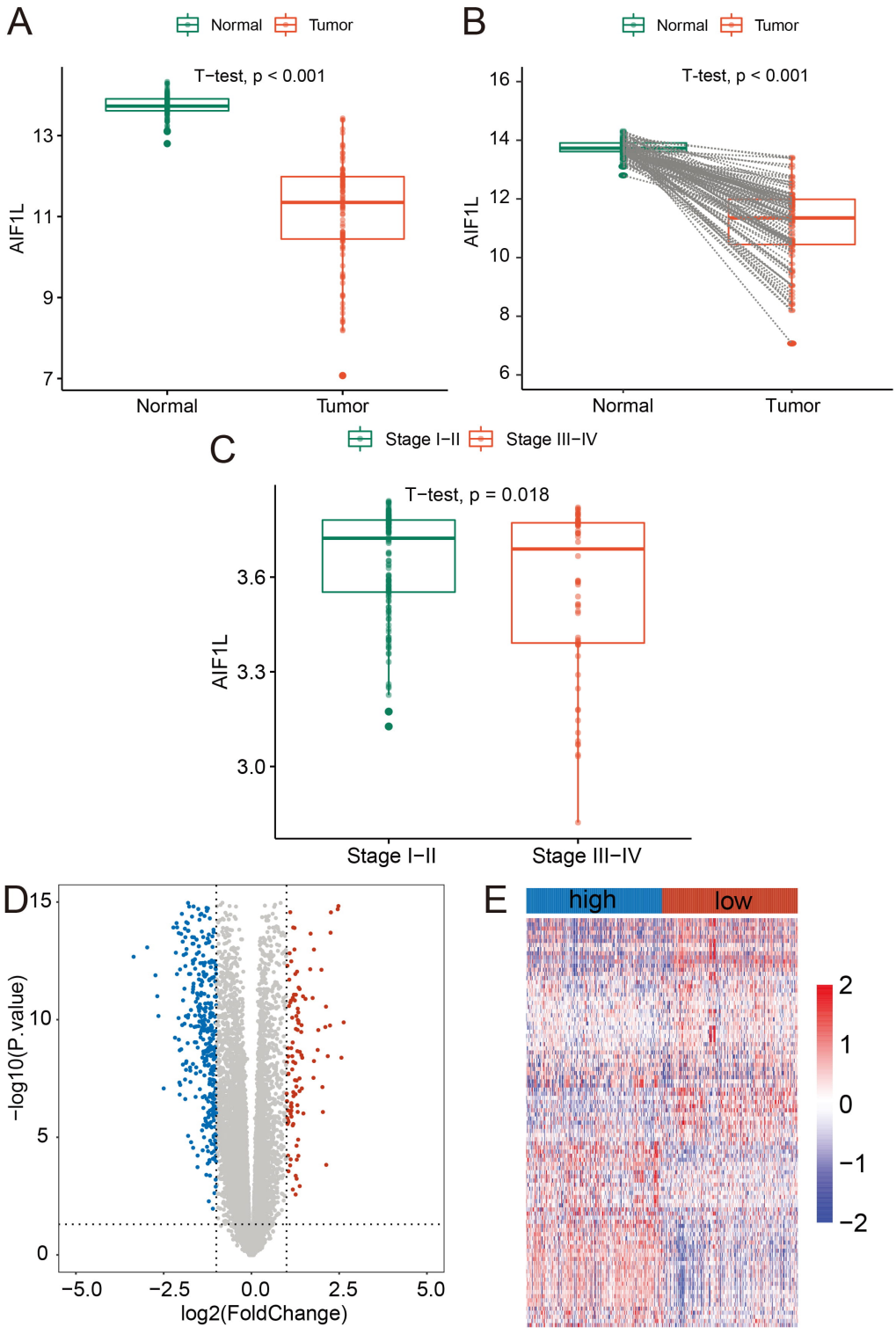

Fig. 2. Validation in an independent dataset and DEG analysis. (A) Students *t*-test result for *AIF1L* expression between ccRCC and normal kidney samples. (B) Paired *t*-test result for *AIF1L* expression between paired ccRCC and normal kidney samples. (C) Students *t*-test result for *AIF1L* expression in Stage I–II and Stage III–IV samples. (D) Volcano plot visualizing the DEGs. The data for 539 ccRCC samples and 72 corresponding healthy kidney samples was extracted from the TCGA datase. The vertical lines demarcate the log2 fold-change values, while the horizontal line marks a –log10 *p*-value of 0.05. Red represents the upregulated genes, while blue represents the downregulated genes. (E) Heatmap for the DEGs. The data for 539 ccRCC samples and 72 corresponding healthy kidney samples was extracted from the TCGA datase. The samples were divided into two groups based on the median value for *AIF1L* expression. Abbreviations: DEG, differently expressed genes.

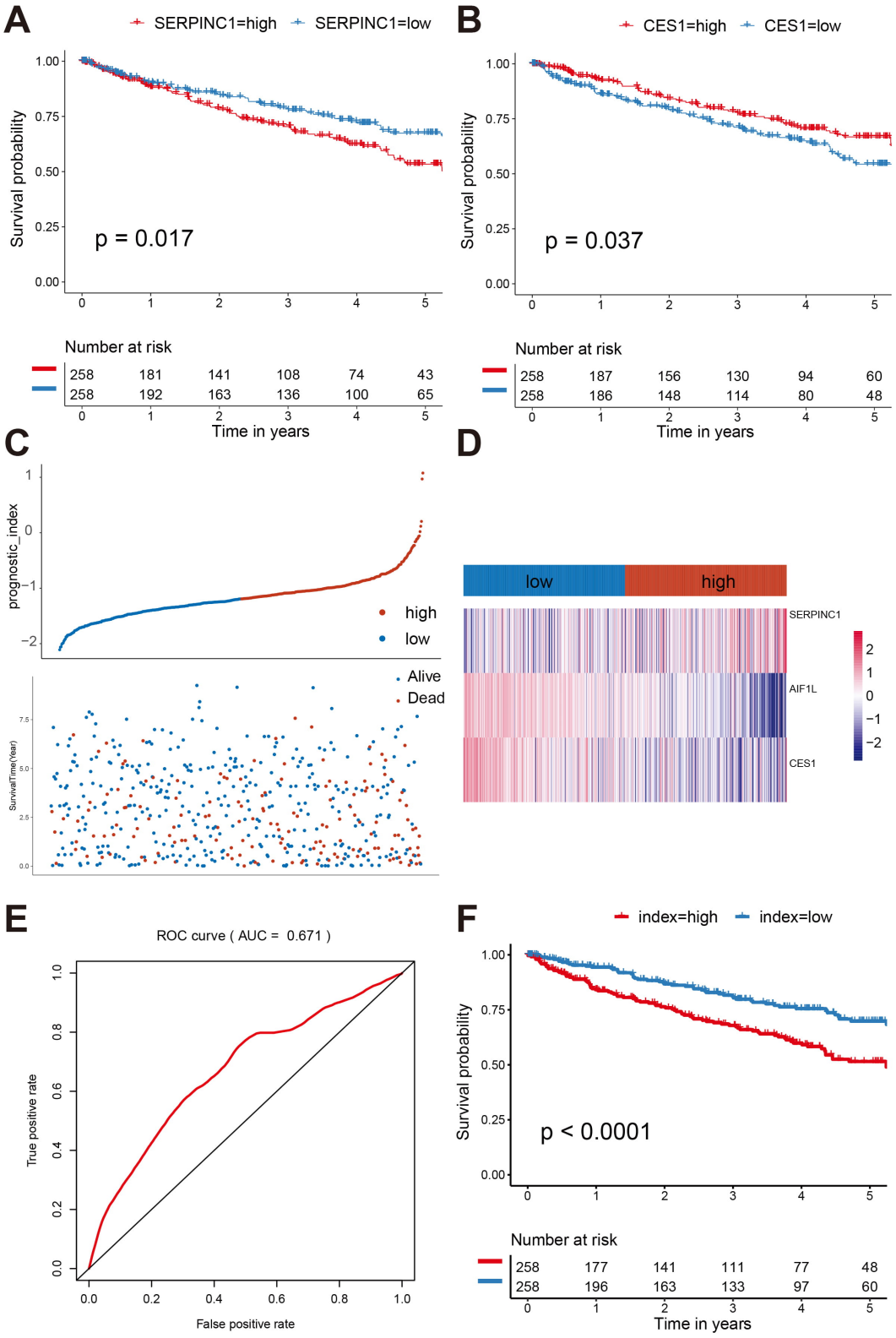

Fig. 3. Construction of a prognostic index model based on the expression level of three genes (*AIF1L*, *SERPINC1*, and *CES1*). (A–B) Kaplan-Meier survival plots for *SERPINC1* and *CES1*. High expression of *SERPINC1* and low expression of *CES1* indicated a poorer prognosis. (C) Detailed information on the low and high prognostic index groups in the TCGA dataset (upper); survival status and survival time for the TCGA ccRCC cohort (lower). (D) Heatmap for *AIF1L*, *SERPINC1*, and *CES1* expression in the TCGA dataset. (E) ROC curve estimating the performance of the prognostic index model for predicting first-year survival in the TCGA dataset. (F) Kaplan-Meier survival plots for high- and low-risk groups in the TCGA dataset.

chosen to validate these results. Students *t*-test and paired *t*-tests confirmed the high expression level of *AIF1L* in normal kidney tissue compared to ccRCC samples in the independent GSE40435 dataset (p-value < 0.001, Fig. 2A–B). Based on the stages of ccRCC samples from GSE40435 dataset, *AIF1L* expression was also significantly higher in stage I–II tumors compared to stage III–IV tumors (p-value = 0.018, Fig. 2C). Taken together, these results indicate that downregulation of *AIF1L* expression correlates with malignancy, advanced tumor stage, and worse patient survival.

3.2 DEGs analysis between AIF1L-high and AIF1L-low groups in TCGA dataset

The data for 539 ccRCC samples and 72 corresponding healthy kidney samples was extracted from the TCGA dataset. The median value for *AIF1L* expression was used to obtain high- and low-expression *AIF1L* groups. In total, 766 DEGs were identified using "edgeR", comprising 165 increased and 601 decreased DEGs in the *AIF1L*-high group (Fig. 2D). A heatmap was then plotted to reveal the top 50 increased expression and top 50 decreased expression genes (Fig. 2E).

3.3 Enrichment analysis

GO and KEGG enrichment analyses were conducted to identify involved pathways for the DEGs. Cellular Component (CC) enrichment analysis revealed the DEGs were mainly enriched in signaling pathways such as "collagen-containing-extracellular-matrix", "blood-microparticle", "endoplasmic-reticulum-lumen", and "high-density-lipoprotein-particle" (Table 1). In Biological Process (BP), the DEGs were mainly involved in response pathways such as the "humoral-immune-response", "antimicrobial-humoral-response", "negative-regulation-of-peptidase", "hormone-metabolic-process", and "negative-regulation-of-endopeptidase-activity". In Molecular Function (MF), the DEGs were mainly involved in inhibitor and binding activities such as "peptidase-inhibitor-activity", "endopeptidase-inhibitor-activity", "serine-type endopeptidase-inhibitor activity", and "endopeptidase-regulator-activity". KEGG pathway analysis of DEGs further revealed immune-related pathways and metabolism-related pathways such as "complement-and-coagulation-cascades", "retinol-metabolism" and "metabolism-of-xenobiotics-by cytochrome-P450" signaling pathways (Table 2).

3.4 Construction of a prognostic model incorporating novel biomarkers

Univariate and multivariate Cox regression analysis was used to evaluate the prognostic significance of DEGs. Three genes (*AIF1L*, *SERPINC1*, and *CES1*) were selected by this analysis. The hazard ratio (HR) and 95% confidence interval (CI) for these were: *AIF1L* (HR = 0.83, 95% CI: 0.76–0.91), *SERPINC1* (HR = 1.33, 95% CI: 1.12–1.58), and *CES1* (HR = 0.87, 95% CI: 0.78–0.97). Kaplan-Meier survival analysis revealed that high *SERPINC1* expression and low *CES1* expression were associated with worse prognosis (Fig. 3A–B). Given their significant association with prognosis, *AIF1L*, *SERPINC1* and CES were regarded as prognosis-related mRNA signatures in order to develop a prognostic index model. The prognostic index of each patient sample was calculated as follows: prognostic index = (–0.17) × *AIF1L* + (0.28) × *SERPINC1* + (–0.13) × *CES1*. The detailed prognostic index, survival status, and mRNA expression values for the three genes are shown in Fig. 3C–D. The performance of the prognostic index model for predicting the first-year survival rate of patients from the TCGA-ccRCC dataset was revealed by AUC analysis to be 0.671 (Fig. 3E). Kaplan-Meier survival analysis showed that patients with a high prognostic index had worse overall survival (Fig. 3F).

4. Discussion

Metastasis is found in 25–30% of ccRCC patients at the initial diagnosis [29,30]. Tumor metastasis results in death in >90% of cases and is thus associated with worse patient prognosis [31]. Cancer cells show an inherent ability to migrate, invade adjacent tissues and enter the vasculature, and thus to eventually metastasize. They crawl along extracellular matrix (ECM) fibers toward blood vessels in the primary tumor. By expanding their pseudopodia, the cancer cells generate a force that pulls the cell body forward and drives cell migration along the fibers at the migration front [32].

EF-hand (EFh) domain-containing proteins are associated with numerous disease states, including chronic inflammation and tumor progression [12]. The *AIF1L* protein structure encompasses two central EFh motifs that lack bound Ca^{2+} [18]. *AIF1L* is expressed at high levels in kidney tissues. Previous research has suggested potential associations between *AIF1L* and podocytes. Other studies have revealed extensive accumulation of *AIF1L* within discrete filopodial protrusions [33]. It is well known that filopodia are associated with migration from the primary tumor, degradation of the basal layer, and intravascular infiltration [34]. *AIF1L* has been reported to inhibit the migration and invasion of breast cancer cells by regulating actin remodeling, with low expression of *AIF1L* being associated with poor prognosis [35]. We reached a similar conclusion in the present study of ccRCC samples. *AIF1L* expression was markedly decreased in ccRCC tissues compared to normal kidney samples. Moreover, the *AIF1L* expression level decreased as the tumor stage increased.

This study also identified two DEGs, *SERPINC1* and *CES1*, that are related to *AIF1L*. Results from the TCGA/GEO dataset and validation of gene expression and survival differences confirmed the prognostic significance of *SERPINC1* and *CES1* in ccRCC. *SERPINC1* (serpin peptidase inhibitor clade C member 1), also referred to as an-

Table 1. Gene Ontology (GO) enrichment analysis of DEGs.

ID	Description	*p* value	Count	Type
GO:0062023	collagen-containing extracellular matrix	<0.001	57	CC
GO:0072562	blood microparticle	<0.001	33	CC
GO:0005788	endoplasmic reticulum lumen	<0.001	40	CC
GO:0034364	high-density lipoprotein particle	<0.001	10	CC
GO:0042627	chylomicron	<0.001	7	CC
GO:0006959	humoral immune response	<0.001	50	BP
GO:0019730	antimicrobial humoral response	<0.001	26	BP
GO:0010466	negative regulation of peptidase activity	<0.001	34	BP
GO:0042445	hormone metabolic process	<0.001	31	BP
GO:0010951	negative regulation of endopeptidase activity	<0.001	33	BP
GO:0030414	peptidase inhibitor activity	<0.001	31	MF
GO:0004866	endopeptidase inhibitor activity	<0.001	30	MF
GO:0004867	serine-type endopeptidase inhibitor activity	<0.001	22	MF
GO:0061135	endopeptidase regulator activity	<0.001	30	MF
GO:0005539	glycosaminoglycan binding	<0.001	32	MF

Table 2. Kyoto Encyclopedia of Genes and Genomes (KEGG) enrichment analysis of DEGs.

ID	Description	*p* value	Count
hsa04610	Complement and coagulation cascades	<0.001	23
hsa00830	Retinol metabolism	<0.001	17
hsa00140	Steroid hormone biosynthesis	<0.001	14
hsa04976	Bile secretion	<0.001	16
hsa00980	Metabolism of xenobiotics by cytochrome P450	<0.001	14
hsa00982	Drug metabolism-cytochrome P450	<0.001	13
hsa04979	Cholesterol metabolism	<0.001	10
hsa05204	Chemical carcinogenesis-DNA adducts	<0.001	11
hsa04974	Protein digestion and absorption	<0.001	13

tithrombin III (ATIII) [36], regulates coagulation by inhibiting various factors and also has anti-inflammatory effects on epithelial cells [37]. Previous studies have reported that *SERPINC1* expression is upregulated in nasopharyngeal carcinoma tissue [37], bladder cancer tissue [37], endometrial and exosome cancer tissue [38] compared to adjacent normal tissues. *SERPINC1* expression was also strongly associated with the development occurrence and progression of certain tumor types [39–41] and has been identified as an immune-related gene. *SERPINC1* expression is prognostic for the survival of lung adenocarcinoma41, uveal melanoma [40] and hepatocellular carcinoma [41] patients. *CES1*, also referred to as serine esterase 1, is protective against xenobiotics and is primarily expressed in the epithelia of metabolic organs including the liver, lungs and bladder [42,43]. The restrain of *CES1* in mononuclear cells display a diminished ability to lyse cancer cells [42]. Deficient *CES1* enzyme activity was also frequently observed in non-Hodgkin lymphoma and B-cell chronic lymphocytic leukemia [42,43], suggesting a possible cancer-cell-killing or cancer monitoring function for *CES1*.

To our knowledge, this is the first report of potential prognostic value for *AIF1L*, *SERPINC1*, and *CES1* expression in ccRCC patients. The prognostic index model based on the three genes revealed a better performance than each gene alone. The performance of this model for the prediction of first-year survival in the TCGA dataset reached 0.671 using AUC analysis, indicating that it can predict the prognosis of ccRCC patients. One limitation of this study is that the model's risk score was not compared with other clinical parameters (age, histological grade, and pathological stage) for the prediction of overall survival. Furthermore, this research was conducted using retrospective data available from public databases. Further verification will require prospective clinical trials.

5. Conclusions

AIF1L expression is markedly decreased in ccRCC tissues compared to normal kidney tissues. The expression level of *AIF1L* decreases with increasing tumor stage. A novel prognostic index model based on *AIF1L*, *SERPINC1* and *CES1* expression can predict the prognosis of ccRCC

patients. This study provides additional insight into the potential role of *AIF1L* in the development and progression of ccRCC. Our proposed prognostic index model may help physicians in assessing the prognosis of ccRCC patients.

Abbreviations

RCC, renal cell carcinoma; ccRCC, cell renal cell carcinoma; PRCC, papillary RCC; ChRCC, chromophobe RCC; VEGF, vascular endothelial growth factor; VEGFRs, vascular endothelial growth factor receptors; PD-1, programmed death 1; EFh, EF-hand; *AIF1*, allograft inflammatory factor 1; *AIF1L*, allograft inflammatory factor 1 like; FPKM, Fragments Per Kilobase Million; TPM, Transcripts Per Kilobase Million; GEO, Gene Expression Omnibus; DEGs, differentially expressed genes; GO, Gene Ontology; KEGG, Kyoto Encyclopedia of Genes and Genomes; K-M, Kaplan-Meier; AUC, area under the ROC curve; HR, hazard ratio; CI, confidence intervals; ECM, extracellular matrix; *SERPINC1*, serpin peptidase inhibitor clade C member 1; ATIII, antithrombin III.

Author contributions

Dataset downloading and analyses—SZ, ZC, JC, MS, YC. Conception and Design—AY, RL, SZ, JL, FL. Manuscript writing—YW, YX, JZ, WC, HW. Manuscript revision—HW, JL, FF, ZW, CW, BX. All authors contributed to editorial changes in the manuscript. All authors read and approved the final manuscript.

Ethics approval and consent to participate

Not applicable.

Acknowledgment

Not applicable.

Funding

This work was supported by grants from the Natural Science Foundation of Zhejiang Province (LQ20H160007), the Natural Science Foundation of Fujian Province (2019J01153), the fourth batch of key discipline construction Project fund of Fujian Medical University Union Hospital, and Startup Fund for scientific research, Fujian Medical University (2019QH1053).

Conflict of interest

The authors declare no conflict of interest.

Availability of data and materials

The datasets supporting the conclusions of this article are included in this article.

References

[1] Capitanio U, Bensalah K, Bex A, Boorjian SA, Bray F, Coleman J, *et al*. Epidemiology of Renal Cell Carcinoma. European Urology. 2019; 75: 74–84.

[2] Ferlay J, Colombet M, Soerjomataram I, Parkin DM, Piñeros M, Znaor A, Bray F. Cancer statistics for the year 2020: an overview. International Journal of Cancer. 2021; 149: 778–789.

[3] Zhou Y, Zhang R, Ding Y, Wang Z, Yang C, Tao S, *et al*. Prognostic nomograms and Aggtrmmns scoring system for predicting overall survival and cancer-specific survival of patients with kidney cancer. Cancer Medicine. 2020; 9: 2710–2722.

[4] Hadoux J, Vignot S, De La Motte Rouge T. Renal Cell Carcinoma: Focus on Safety and Efficacy of Temsirolimus. Clinical Medicine Insights: Oncology. 2010; 4: 143–154.

[5] Motzer RJ, Tannir NM, McDermott DF, Arén Frontera O, Melichar B, Choueiri TK, *et al*. Nivolumab plus Ipilimumab versus Sunitinib in Advanced Renal-Cell Carcinoma. New England Journal of Medicine. 2018; 378: 1277–1290.

[6] Powles T, Plimack ER, Soulières D, Waddell T, Stus V, Gafanov R, *et al*. Pembrolizumab plus axitinib versus sunitinib monotherapy as first-line treatment of advanced renal cell carcinoma (KEYNOTE-426): extended follow-up from a randomised, open-label, phase 3 trial. The Lancet Oncology. 2020; 21: 1563–1573.

[7] Grünwald V, Hadaschik B. Re: Nivolumab plus Cabozantinib Versus Sunitinib for Advanced Renal-cell Carcinoma. European Urology. 2021; 80: 256–257.

[8] Hindié E. Lenvatinib plus Pembrolizumab for Renal Cell Carcinoma. New England Journal of Medicine. 2021; 385: 287.

[9] Atkins MB, Tannir NM. Current and emerging therapies for first-line treatment of metastatic clear cell renal cell carcinoma. Cancer Treatment Reviews. 2018; 70: 127–137.

[10] Makhov P, Joshi S, Ghatalia P, Kutikov A, Uzzo RG, Kolenko VM. Resistance to Systemic Therapies in Clear Cell Renal Cell Carcinoma: Mechanisms and Management Strategies. Molecular Cancer Therapeutics. 2018; 17: 1355–1364.

[11] Turajlic S, Xu H, Litchfield K, Rowan A, Chambers T, Lopez JI, *et al*. Tracking Cancer Evolution Reveals Constrained Routes to Metastases: TRACERx Renal. Cell. 2018; 173: 581–594.e12.

[12] Zhang Y, Wang S, Li L. EF Hand Protein IBA2 Promotes Cell Proliferation in Breast Cancers via Transcriptional Control of Cyclin D1. Cancer Research. 2016; 76: 4535–4545.

[13] Jia J, Bai Y, Fu K, Sun Z, Chen X, Zhao Y. Expression of allograft inflammatory factor-1 and CD68 in haemangioma: implication in the progression of haemangioma. British Journal of Dermatology. 2008; 159: 811–819.

[14] Deininger MH, Seid K, Engel S, Meyermann R, Schluesener HJ. Allograft inflammatory factor-1 defines a distinct subset of infiltrating macrophages/microglial cells in rat and human gliomas. Acta Neuropathologica. 2000; 100: 673–680.

[15] Li T, Feng Z, Jia S, Wang W, Du Z, Chen N, *et al*. Daintain/AIF-1 promotes breast cancer cell migration by up-regulated TNF-α via activate p38 MAPK signaling pathway. Breast Cancer Research and Treatment. 2012; 131: 891–898.

[16] Liu S, Tan W, Chen Q, Chen X, Fu K, Zhao Y, *et al*. Daintain/AIF-1 promotes breast cancer proliferation via activation of the NF-κB/cyclin D1 pathway and facilitates tumor growth. Cancer Science. 2008; 99: 952–957.

[17] Jia J, Cai Y, Wang R, Fu K, Zhao Y. Overexpression of Allograft Inflammatory Factor-1 Promotes the Proliferation and Migration of Human Endothelial Cells (HUV-EC-C) Probably by up-Regulation of Basic Fibroblast Growth Factor. Pediatric Research. 2010; 67: 29–34.

[18] Ye Y, Miao S, Lu R, Xia X, Chen Y, Zhang J, *et al*. Allograft inflammatory factor-1 is an independent prognostic indicator that regulates β-catenin in gastric cancer. Oncology Reports. 2014; 31: 828–834.

[19] Schulze JO, Quedenau C, Roske Y, Adam T, Schüler H, Behlke

J, *et al*. Structural and functional characterization of human Iba proteins. FEBS Journal. 2008; 275: 4627–4640.
[20] Chen ZW, Ahren B, Ostenson CG, Cintra A, Bergman T, Moller C, *et al*. Identification, isolation, and characterization of daintain (allograft inflammatory factor 1), a macrophage polypeptide with effects on insulin secretion and abundantly present in the pancreas of prediabetic BB rats. Proceedings of the National Academy of Sciences. 1997; 94: 13879–13884.
[21] Shyamsundar R, Kim YH, Higgins JP, Montgomery K, Jorden M, Sethuraman A, *et al*. A DNA microarray survey of gene expression in normal human tissues. Genome Biology. 2005; 6: R22.
[22] Autieri MV. CDNA Cloning of Human Allograft Inflammatory Factor-1: Tissue Distribution, Cytokine Induction, and mRNA Expression in Injured Rat Carotid Arteries. Biochemical and Biophysical Research Communications. 1996; 228: 29–37.
[23] Utans U, Arceci RJ, Yamashita Y, Russell ME. Cloning and characterization of allograft inflammatory factor-1: a novel macrophage factor identified in rat cardiac allografts with chronic rejection. Journal of Clinical Investigation. 1995; 95: 2954–2962.
[24] Wozniak MB, Le Calvez-Kelm F, Abedi-Ardekani B, Byrnes G, Durand G, Carreira C, *et al*. Integrative genome-wide gene expression profiling of clear cell renal cell carcinoma in Czech Republic and in the United States. PLoS ONE. 2013; 8: e57886.
[25] Robinson MD, McCarthy DJ, Smyth GK. EdgeR: a Bioconductor package for differential expression analysis of digital gene expression data. Bioinformatics. 2010; 26: 139–140.
[26] Lin H, Chen L, Li W, Chen Z. Novel Therapies for Tongue Squamous Cell Carcinoma Patients with High-Grade Tumors. Life. 2021; 11: 813.
[27] Yu G, Wang LG, Han Y, He QY. ClusterProfiler: an R Package for Comparing Biological Themes among Gene Clusters. OMICS. 2012; 16: 284–287.
[28] Lin H, Zelterman D. Modeling Survival Data: Extending the Cox Model. Technometrics. 2002; 44: 85–86.
[29] Xu W, Xu Y, Wang J, Wan F, Wang H, Cao D, *et al*. Prognostic value and immune infiltration of novel signatures in clear cell renal cell carcinoma microenvironment. Aging. 2019; 11: 6999–7020.
[30] Ganesh K, Massagué J. Targeting metastatic cancer. Nature Medicine. 2021; 27: 34–44.
[31] Yamaguchi H, Condeelis J. Regulation of the actin cytoskeleton in cancer cell migration and invasion. Biochimica et Biophysica Acta-Molecular Cell Research. 2007; 1773: 642–652.
[32] Yasuda-Yamahara M, Rogg M, Yamahara K, Maier JI, Huber TB, Schell C. *AIF1L* regulates actomyosin contractility and filopodial extensions in human podocytes. PLoS ONE. 2018; 13: e200487.
[33] Arjonen A, Kaukonen R, Ivaska J. Filopodia and adhesion in cancer cell motility. Cell Adhesion & Migration. 2014; 5: 421–430.
[34] Liu P, Li W, Hu Y, Jiang Y. Absence of *AIF1L* contributes to cell migration and a poor prognosis of breast cancer. OncoTargets and Therapy. 2018; 11: 5485–5498.
[35] Caspers M, Pavlova A, Driesen J, Harbrecht U, Klamroth R, Kadar J, *et al*. Deficiencies of antithrombin, protein C and protein S –Practical experience in genetic analysis of a large patient cohort. Thrombosis and Haemostasis. 2017; 108: 247–257.
[36] Xu J, Ying Y, Xiong G, Lai L, Wang Q, Yang Y. Knockdown of serpin peptidase inhibitor clade C member 1 inhibits the growth of nasopharyngeal carcinoma cells. Molecular Medicine Reports. 2019; 19: 3658–3666.
[37] Ura B, Biffi S, Monasta L, Arrigoni G, Battisti I, Di Lorenzo G, *et al*. Two Dimensional-Difference in Gel Electrophoresis (2D-DIGE) Proteomic Approach for the Identification of Biomarkers in Endometrial Cancer Serum. Cancers. 2021; 13: 3639.
[38] Zhao M, Li M, Chen Z, Bian Y, Zheng Y, Hu Z, *et al*. Identification of immune-related gene signature predicting survival in the tumor microenvironment of lung adenocarcinoma. Immunogenetics. 2020; 72: 455–465.
[39] Xie J, Wu Z, Xu X, Liang G, Xu J. Screening and identification of key genes and pathways in metastatic uveal melanoma based on gene expression using bioinformatic analysis. Medicine. 2020; 99: e22974.
[40] Xu X, Zhou Y, Miao R, Chen W, Qu K, Pang Q, *et al*. Transcriptional modules related to hepatocellular carcinoma survival: co-expression network analysis. Frontiers of Medicine. 2016; 10: 183–190.
[41] Taketani M, Shii M, Ohura K, Ninomiya S, Imai T. Carboxylesterase in the liver and small intestine of experimental animals and human. Life Sciences. 2007; 81: 924–932.
[42] Ke CC, Chen LC, Yu CC, Cheng WC, Huang CY, Lin VC, *et al*. Genetic Analysis Reveals a Significant Contribution of *CES1* to Prostate Cancer Progression in Taiwanese Men. Cancers. 2020; 12: 1346.
[43] McCormick JA, Markey GM, Morris TCM, Auld PW, Alexander HD. Lactoferrin inducible monocyte cytotoxicity defective in esterase deficient monocytes. British Journal of Haematology. 1991; 77: 287–290.